Neurogenesis of Rhesus adipose stromal cells

Soo Kyung Kang[1,3], Lorna A. Putnam[1], Joni Ylostalo[3], Ion Razvan Popescu[5], Jason Dufour[2], Andrei Belousov[5] and Bruce A. Bunnell[1,3,4,*]

[1]Division of Gene Therapy and [2]Division of Veterinary Medicine, Tulane National Primate Research Center, Tulane University Health Sciences Center, 18703 Three Rivers Road, Covington, LA 70433, USA
[3]Center of Gene Therapy, [4]Department of Pharmacology, Tulane University Health Sciences Center and [5]Department of Cell and Molecular Biology, Tulane University, New Orleans, LA 70112, USA
*Author for correspondence (e-mail: bbunnell@tulane.edu)

Accepted 13 April 2004
Journal of Cell Science 117, 4289-4299 Published by The Company of Biologists 2004
doi:10.1242/jcs.01264

Summary

In this study, we isolated and characterized a population of non-human primate adipose tissue stromal cells (pATSCs) containing multipotent progenitor cells. We show that these pATSCs can differentiate into several mesodermal lineages, as well as neural lineage cells. For neural induction of pATSCs and non-human primate bone marrow stromal cells (pBMSCs), the cells were cultured in Neurobasal (NB) media supplemented with B27, basic fibroblast growth factor (bFGF), brain-derived neurotrophic factor (BDNF) and epidermal growth factor (EGF). After 4 days in culture, the pATSCs form compact, spheroid bodies that ultimately become neurospheres (NS). Free-floating neurospheres undergo extensive differentiation when cultured on PDL-laminin. Our data suggest that the neurogenic potential of pATSCs is markedly higher than that of pBMSCs. We have also performed microarray analysis and characterized the gene expression patterns in undifferentiated pATSCs. The direct comparison of gene expression profiles in undifferentiated pATSCs and pATSC-NS, and delineated specific members of important growth factor, signaling, cell adhesion and transcription factors families. Our data indicate that adipose tissue may be an alternative source of stem cells for therapy of central nervous system (CNS) defects.

Supplemental data available online

Key words: Stem cell, Adipose tissue, Neural differentiation, Neurosphere, Non-human primate, Microarray

Introduction

Stem cells are clonogenic cells that have the capacity for self-renewal and multilineage differentiation. During embryogenesis, totipotent embryonic stem cells that are derived from the blastocyst give rise to ectoderm, mesoderm and endoderm lineage cell populations (Weissman, 2000). It has become evident that stem cells persist in adult tissues, although they represent a rare population localized in small niches (Woodbury et al., 2002). Adult stem cells are not totipotent, but they are capable of self-renewal and differentiation into multiple specialized cell types (Kopen et al., 1999). In tissues from postnatal animals, stem cells have been successfully isolated from liver, intestine, bone marrow and brain (Wei et al., 2000). Neural precursors that differentiate into neurons, astrocytes and oligodendrocytes may hold significant therapeutic potential for the replacement of damaged or diseased neural tissue resulting from congenital neuropathological conditions, brain injuries and neurodegenerative disorders. Although regional neurogenesis continues throughout the lifespan of rodents and humans, the number and availability of neural stem cells (NSCs) is limited in the postnatal central nervous system (CNS) (Barami et al., 2001; Shetty and Turner, 1996). The transplantation of NSCs has been shown to provide functional improvement in vivo (Barami et al., 2001; Borlongan et al., 1997; Masada et al., 1997; Shetty and Turner, 1996).

Recent evidence indicates that bone marrow stem cell transplantation effectively prevented the progression of neurological disease signs in some functional studies, if it is performed at an early stage in the disease (Jin et al., 2002). Subpopulations of bone marrow cells may serve as an alternative source of stem cells for the treatment of CNS disease, whereby mesenchymal stem cells differentiate into various lineages of brain cells. It has been shown that cells isolated from both bone marrow and umbilical cord blood (CB) can give rise to neural cells in vitro (Black and Woodbury, 2001; Kohyama et al., 2001; Reyes and Verfaillie, 2001; Deng et al., 2001; Sanchez-Ramos et al., 2000; Sanchez-Ramos et al., 2001; Woodbury et al., 2000; Colter et al., 2000; Colter et al., 2001) and in vivo (Azizi et al., 1998; Kopen et al., 1999; Mezey et al., 2000; Brazelton et al., 2000). Many studies have shown that bone marrow-derived cells can give rise to neural cells as well as many tissue-specific cell phenotypes, including hematopoietic, skeletal muscle, hepatic, heart and vascular endothelial cells (Terskikh et al., 2001; Gussoni et al., 1999; Petersen et al., 1999). The results of these studies have shown that host tissue-specific microenvironment conditions may be essential for the multilineage transdifferentiation of bone marrow-derived stem cells (BMSCs). BMSCs also have been used as vehicles for gene delivery to various tissues including the brain (Ding et al., 1999; Jin et al., 2002; Park et al., 2001; Suzuki et al., 2000; Kang et al., 2003). These findings suggest that bone marrow cells are a potential source of brain progenitor cells and have clinical importance in applications for tissue engineering and also as vehicles for gene therapy.

Adipose tissue has been identified as an alternative source of pluripotent mesenchymal stromal cells (Patrick, 2000; Zuk et al., 2001). Cells isolated from adipose tissue are self-renewing and can be induced to differentiate along several mesenchymal tissue lineages, including adipocytes, osteoblasts, myocytes and chondrocytes (Zuk et al., 2001; Halvorsen et al., 2001; Erickson et al., 2002). Adipose tissue, like bone marrow, is derived from the embryonic mesoderm and contains a heterogeneous stromal cell population (Zuk et al., 2002). Recently, MSCs isolated from the adipose tissue of rats were differentiated into neuron-like cells expressing neuronal markers (Kang et al., 2003; Safford et al., 2002). Therefore, adipose tissue may serve as an alternative source of pluripotent stromal cells capable of neural differentiation and, as such, may have application for the treatment of neurologic disorders.

Because little is known about the biologic, differentiation or engraftment properties of mesenchymal stem cells in higher order animals, we have begun to isolate and characterize the biological properties of these cells from the adipose tissue of rhesus monkeys. Macaques share greater biological similarities with humans than most other species with which stem cell research is being conducted, and therefore provide an unmatched opportunity to research diseases that afflict humans. The goals of these studies were as follows: (1) to isolate and characterize the growth and mesodermal differentiation capabilities of adipose tissue stem cells compared with pBMSC and (2) to investigate the differentiation potential of these cells along neural lineages in vitro. Our results show that adipose tissue is a viable source of mesenchymal stem cells in non-human primates that are capable of multilineage differentiation along mesodermal and neural lineages in vitro.

Materials and Methods

Animals

All animal procedures conformed to the requirements of the Animal Welfare Act and protocols were approved before implementation by the Institutional Animal Care and Use Committee (IACUC) of Tulane University. The animals were housed under conditions approved by the Association for the Assessment and Accreditation of Laboratory Animal Care International. Healthy Rhesus monkeys (*Macaca mulatta*, 15-20 kg, 10 to 15 years old) of both sexes were used for these studies. Activities related to animal care were performed as per standard Tulane National Primate Research Center operating procedures. All animals were negative for simian retrovirus (SRV) and simian T cell leukemia virus (STLV).

Isolation and culture of stromal cells

Non-human primate adipose tissue was obtained under local anesthesia. The raw adipose tissue was processed according to established methodologies to obtain a stromal vascular fraction (Zuk et al., 2002). To isolate stromal cells, samples were washed extensively with equal volumes of phosphate-buffered saline (PBS), and digested at 37°C for 30 minutes with 0.075% collagenase (Sigma, St Louis, MO). Enzyme activity was neutralized with α-Modified Eagle's Medium (MEM) (Invitrogen, Gaithersburg, MD), containing 10% FBS and centrifuged at 1200 ***g*** for 10 minutes to obtain a high-density cell pellet. The pellet was resuspended in red blood cell (RBC) lysis buffer (Biowhittaker, Walkersville, MD) and incubated at room temperature for 10 minutes to lyse contaminating RBCs. The stromal cell pellet was collected by centrifugation, as described above, and incubated overnight at 37°C/5% CO_2 in α-MEM medium containing 10% FBS.

For neural lineage potential comparison studies, rhesus BMSCs were obtained from 2-3 ml aspirates from the femur. The aspirate was diluted 1:2 in PBS and marrow cell fraction was obtained by centrifugation over 50% Percoll (Pharmacia LKB, Piscataway, NJ) at 1100 ***g*** for 30 minutes at 20°C. The nucleated cells were collected from the interface, diluted with two volumes of PBS, and collected by centrifugation at 900 ***g***. The cells were resuspended, counted and plated at a concentration of 150-200 cells/cm^2 onto Nunclon culture dish (Nunc, Naperville, IL). The cells were cultured in α-MEM supplemented with 10% FBS (Atlanta Biological, Lawrenceville, GA) and 1% penicillin/streptomycin antibiotic solution. Medium was replaced first at 24 hours and then every third day thereafter.

Confirmation of mesodermal lineage differentiation of pATSC

To verify the multipotential differentiation of mesenchymal characteristics of pATSCs, cells were subjected to differentiation in conditions known to induce adipogenic, osteogenic and chondrogenic lineages in human cells. Before culture in the induction medium, cultures were grown to at least 80% confluence.

For adipogenic differentiation, pATSCs were induced by passaging cells at a 1:10 dilution in control medium and supplemented 10 ng/ml insulin and 10^{-9} M dexamethasone. Adipogenic differentiation was visualized by the presence of highly refractive intracellular lipid droplets in phase contrast microscopy or staining by Oil-Red O. To induce osteogenic differentiation, the cultures were fed daily with control medium to which was added 10 mM β-glycerophosphate, 50 ng/ml ascorbic acid and 10^{-9} M dexamethasone for 3 weeks. Mineralization of the extracellular matrix was visualized by staining of the cultures with Alizarin Red S (2% w/v Alizarin Red S adjusted to pH 4 using ammonium hydroxide) for 5 minutes at room temperature followed by a wash with water. Chondroblast differentiation was induced by differentiation medium supplemented with 6.25 μg/ml insulin, 10 ng/ml transofrming growth factor β1 (TGF β1) and 50 ng ascorbate-2-phosphate in control medium for 3-4 weeks. After differentiation, the cultures were washed and fixed in 4% paraformaldehyde and stained for glycosaminoglycans using 0.1% Safranin O.

Generation of neurospheres from pATSC and pBMSC

Undifferentiated pATSCs and pBMSCs cultured at high densities spontaneously formed spherical clumps of cells that were isolated in 0.25% trypsin (Invitrogen). We also collected free floating neurospheres that were released from the cell culture surface into the culture media. The spheres of cells were transferred to a Petri dish and cultured in Neurobasal medium (NB) (Invitrogen) supplemented with B27 (Invitrogen), 20 ng/ml bFGF, and 20 ng/ml EGF (Sigma) for 4-7 days. The culture density of the spheroid bodies was maintained at 10-20 cells/cm^2 to prevent self aggregation.

In vitro differentiation of pATSC to neural cells

For neural lineage differentiation, neurospheres derived from pATSCs were layered on PDL-laminin double-coated chamber slide (Lab Tek, Nalge/Nunc). Spheres were cultured and maintained for 10 days in NB media containing only the B27 supplement. During differentiation, 70% of the media was replaced every 4 days. The cells were examined at 10 days after differentiation by immunocytochemistry, western blot and reverse transcription polymerase chain reaction (RT-PCR). All data to be shown are representative of at least three different experiments.

Flow cytometric analysis of surface epitopes

For phenotypic characterization by flow cytometry, undifferentiated pATSCs, pATSC-derived neurospheres and adherent cells were

Table 1. Primer sequences used in this study

Gene	Forward sequence (5′-3′)	Reverse sequence (5′-3′)
Oct-4	CGC ACC ACT GGC ATT GTC AT	TTC TCC TTG ATG TCA CGC AC
Telomerase	GCA AGT TGC AAA GCA TTG GA	ACC TCT GCT TCC GAC AGC TC
Hes 1	CTA CCT CTC TCC TTG GTC CT	AGG TGC TTC ACT GTC ATT TC
β-actin	TTG TTA CCA ACT GGG ACG ACA TGG	GAT CTT GAT CTT CAT GGT GCT AGG
Nestin	GCC CTG ACC ACT CCA GTT TA	GGA GTC CTG GAT TTC CTT CC
BDNF	GTC ATC GAA GAG CTG CTG GA	CTT TTG TCT ATG CCC CTG CA
MAP2	CAG CAA AGG GAT ACT TTC AC	ATG CTT TTT GTT GCT TCT TC
GAD65	GAA TCT TTT CTC CTG GTG GTG	GAT CAA AAG CCC CGT ACA CAG
GFAP	GCT CGA TCA ACT CAC CGC CAA CA	GGG CAG CAG CGT CTG TCA GGT C
Trk A	TCT TCA CTG AGT TCC TGG AG	TTC TCC ACC GGG TCT CCA GA
Trk B	AGT CCA GAC ACT CAG GAT TTG TAC	CTC CGT GTG ATT GGT AAC ATG
Trk C	CAT CCA TGT GGA ATA CTA CC	TGG GTC ACA GTG ATA GGA GG
P-75	CTG GAC AGC GTG ACG TTC TCC	CTG CCA CCG TGC TGG CTA TGA

harvested by trypsinization, washed twice with PBS and suspended at a concentration of 1×10^6 cell/ml and incubated with antibodies to the following antigens: CD3, CD4, CD8, CD11b, CD13, CD90, CD164, CD133, CD59 and HLA-1 for 20 minutes. For FACS analysis, we used primary antibody directly conjugated with APC, or FITC. Monoclonal antibodies to CD34, CD3, CD4 and CD8 were used to identify cells as hematopoietic. The stained cells were thoroughly washed with two volumes of PBS and fixed in neutralized 2% paraformaldehyde solution. For an isotype control, nonspecific mouse or rabbit IgG (DAKO, Chemicon or Santa Cruz) was substituted for the primary antibody. The labeled cells were analyzed on a FACScan argon laser cytometer (Becton Dickinson, San Jose, CA).

RT-PCR analysis of total cellular RNA

Before and after neural differentiation of pATSCs, total cellular RNA was isolated with Trizol (Invitrogen) reverse transcribed into first strand cDNA using oligo-dT primer and amplified by 35 cycles (94°C, 1 minute; 55°C, 1 minute; 72°C, 1 minute) of PCR using 20 pM of specific primers. PCR amplification was performed using the primer sets. All primer sequences were determined using established human GeneBank sequences for genes indicative of neural lineages or control genes. Duplicate PCR reactions were amplified using primers for GAPDH as a control for assessing PCR efficiency and for subsequent analysis by 1.5% agarose gel electrophoresis.

Primer sequences for all the aforementioned genes were as following (Table 1).

Quantitative real-time RT-PCR

To assess the efficiency of neural differentiation and compare the levels of expression of brain-derived neurotrophic factor (BDNF) and microtubule associated protein-2 (MAP2ab) expression in differentiated pATSCs and pBMSCs, quantification was performed using real-time RT-PCR. Total cellular RNA was isolated using conventional protocol. Human glyceraldehyde-3-phosphate dehydrogenase (GAPDH) primers and probe (5′FAM and 3′TAMRA) were purchased from Applied Biosystems (Foster, CA). Quantitative real-time RT-PCR was performed using this kit according to the manufacturer and an ABI7700 Prism Sequence Detection System. Primer and probe sequences were designed using Primer Express software (PE-Applied Biosystems, Warrington, UK) using gene sequences obtained from the GeneBank database. All probes are designed with a 5′fluorogenic probe 6-FAM and a 3′quencher TAMRA. The expression of human GAPDH was used to standardize gene expression levels.

Immunocytochemistry and FACS analysis of neural differentiated cells

For analysis of neural differentiation of pATSC neurospheres, differentiated cells were fixed with 4% paraformaldehyde, and incubated with 10% goat serum to prevent nonspecific antibody binding. The cells were incubated overnight at 4°C with antibodies. For detection of differentiated neuronal or glial cell proteins, we used several species-specific monoclonal antibodies directed against glial acidic fibrillary protein (GFAP) (1:2000, Dako, Carpinteria, CA), MAP2ab (1:250, Sigma, St Louis, MO), nestin (1:250, Sigma), Neu N (1:500, Sigma), NF160 (1:500, Sigma) and myelin basic protein (MBP) (1:250, Chemicon, Temecula, CA). After extensive washing in PBS, the cells were incubated for 30 minutes with FITC or Alexa Fluor 568 conjugated secondary antibodies (1:250, Molecular Probe, Eugene, OR). Controls in which primary antibodies were omitted or replaced with irrelevant IgG resulted in no detectable staining. Specimens were examined using a Leica TCS SP2 laser scanning microscope equipped with three lasers (Leica Microsystems, Exton, PA). Immunocytochemical studies were repeated at least three times.

Western blot analysis of differentiated cells

Protein extracts were prepared from undifferentiated or differentiated pATSCs by the treatment of lysis buffer containing 20 mM Tris (pH 7.5), 150 mM NaCl, 1 mM EDTA, 1% Triton X-100, 1 mM phenylmethylsulfonylfluoride, 10 μg/ml aprotinin and 1 mM sodium orthovanadate. Total protein (30-40 μg/ml) was resolved on 12.5% acrylamide gel and electroblotted onto Polyvinyldiethylfluoride (PVDF) membrane (Amersham). The blot was probed with either mouse anti-nestin (1:500) or mouse anti-MAP2ab antibodies (1:500). Immunoreactive bands were detected using horseradish peroxidase-conjugated anti-mouse IgG antibodies (Amersham) and visualized by enhanced chemiluminescence (Amersham).

Oligonucleotide microarray analysis

Samples for gene array analysis were prepared from total RNA and microarray analysis was performed following the manufacturer's recommendations. Fragmented cRNA (15 μg) was hybridized 16 hours at 45°C to the HG-U95A array for the comparison study (Affymetrix, Santa Clara, CA). After hybridization, the gene chips were automatically washed and stained with streptavidine-phycoerythrin by using a fluidics station. Finally, the probe arrays were scanned at 3 μm resolution using the Genechip System confocal scanner made for Affymetrix by Agilent. Affymetrix Microarray Suite 4 was used to scan and analyze the relative abundance of each gene as derived from the average difference of intensities. Analysis parameters used by the software were set to values corresponding to moderate stringency. The threshold values to determine the present (P) or absent (A) call were set as follows; $\alpha1=0.05$, $\alpha2=0.065$, $\tau=0.015$. Fluorescence intensity was measured for each chip and normalized to average fluorescence intensity for the entire chip. Output from the microarray analysis was merged with the Unigene or

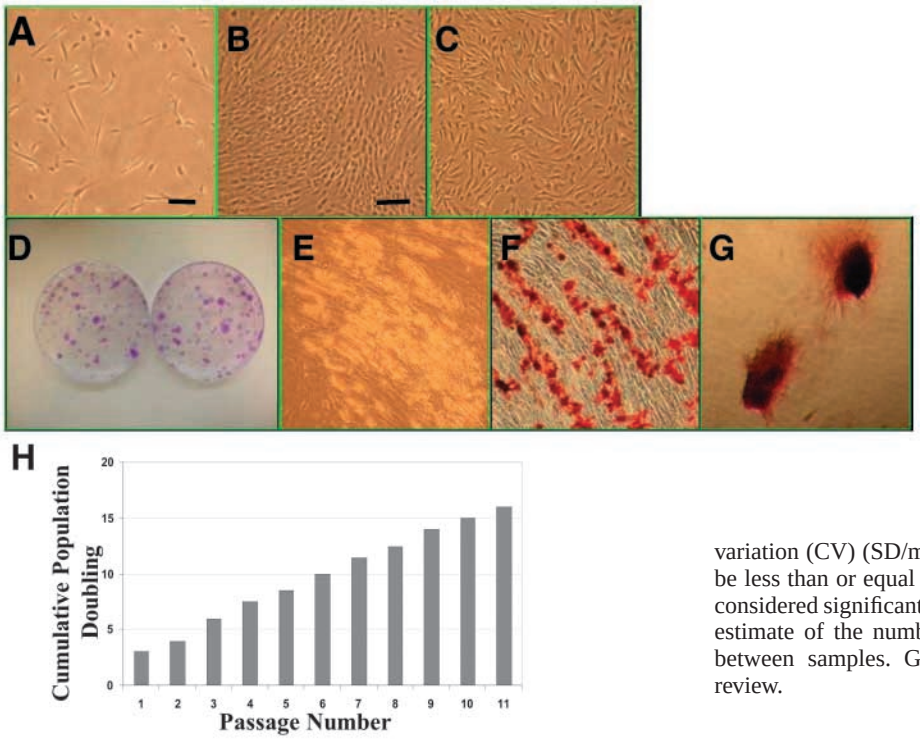

Fig. 1. Morphology and proliferation and differentiation potential of pATSCs. Culture expanded non-human primate ATSCs show the spindle-shaped fibroblastic morphology (A for low density and B for high density). Compared with pATSCs, pBMSCs are more heterogeneous and they have fibroblastic morphology (C). A single cell can be expanded into a clonal population and can generate colony forming units (CFUs) that are shown by Giemsa staining (D). Passage 3-4 pATSCs retain multilineage differentiation capability undergoing adipogenesis (E), osteogenesis (F) and chondrogenesis (G) in vitro. Cumulative population doublings with respect to passage number in multiple animal samples were measured (H). Bars, 40 μm (A); 30 μm (B).

Genebank descriptor and stored as an Excel data spreadsheet. The definition of increase or decrease, or no change of expression for individual genes was based on ranking the Difference Call from two comparisons (2×1), namely, no change (NC) of expression for individual genes was merged with the Unigene or GeneBank descriptor and stored as an Excel data spreadsheet. The definition of increase (I), or no change (NC) of expression for individual genes was based on ranking the Difference Call from the two comparisons (2×1) namely, No change=0, Marginal Increase/Decrease=1/–1, Increase/Decrease=2/–2. The final rank referred to summing up the two values corresponding to the Difference Calls and the value varied from –6 to 6. The cut-off value for the final determination of Increase/Decrease was set as 3/–3. Evaluation of the reproducibility of paired experiments was based on calculation of the coefficient of variation (CV) (SD/mean) for fold change (FC). The CV of FC must be less than or equal to 1.0. Finally, genes with an FC over 1.5 were considered significant. These cut-off values represented a conservative estimate of the numbers of genes whose expression levels differed between samples. Gene categorization was based on a literature review.

Results

Stromal cell morphology characterization

Within two to three passages after the initial plating of the primary culture, pATSCs appeared as a monolayer of broad, flat cells (20-30 mm in diameter) (Fig. 1A). When the cells approached densities over 80%, the cell morphology changed to a more spindle-shaped, fibroblastic morphology (Fig. 1B). pBMSCs isolated from femurs and tibias showed heterogeneous groups of low contrast flat cells together with smaller, more spindle-shaped cells (Fig. 1C). Furthermore, both the pBMSC and pATSC populations had many small, round cells that were attached to or growing on these cells; these might have been cells from the hematopoietic lineage or the recently described rapidly self-renewing stem cells (data

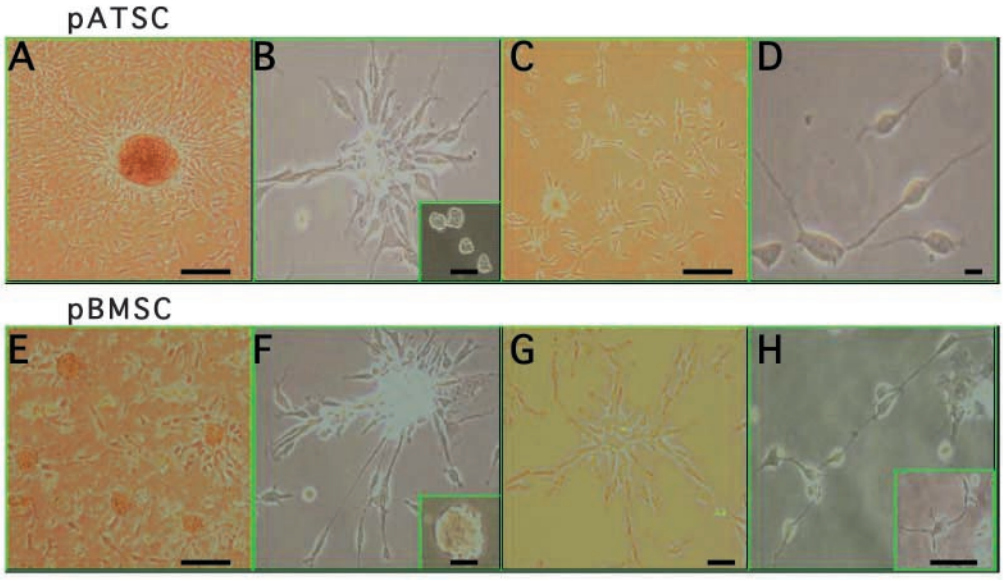

Fig. 2. In vitro differentiation of pATSCs (A-D), pBMSCs (E-H) along neuronal lineages. Stromal cell-derived neurospheres (A,E) cultured in media supplemented with B27, bFGF and EGF for 4-5 days. Free-floating cell spheres in the NB medium (B,F small inset panel). pATSC and pBMSC-derived neurosphere induced differentiation by culturing on the PDL-Laminin-coated substrate for 10-15 days in B27 supplemented NB media (B-D, F-H). Neurospheres attached to the bottom of the culture dish and protrude extensive cell processes (B,C,F,G). The processes became longer and formed diverse networks 10 days after plating (D,H). Bars, 30 μm (A,C,E); 60 μm (B,D,F,G,H).

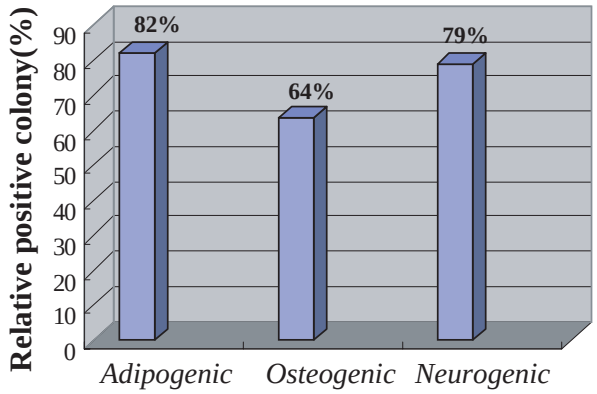

Fig. 3. Evaluation of pATSCs-derived single cell clones pluripotency. Single clones-derived progenies were plated at 50 cells/cm^2 and induced differentiation to adipogenic, osteogenic and neurogenic. After differentiation cells were stained with Oil Red O and Alzarin Red S for detection of fat and mineralization. For neural lineage detection, cells were immunostained with GFAP, Tuj and MBP antibodies. Positive colonies were counted.

not shown) (Colter et al., 2000; Colter et al., 2001). Single-cell pATSC cultures generated CFU (colony forming unit) clones after 2 weeks of culture, indicating the potential for self-renewal (Fig. 1D). For evaluation of pATSCs-derived single-cell clones pluripotency, single clone-derived progenies were plated at 50 cells/cm^2 and induced differentiation to adipogenic, osteogenic and neurogenic. After differentiation cells were stained with Oil Red O and Alzarin Red S to detect fat and calcium deposits. For neural lineage detection, cells were immunostained with GFAP, Tuj and MBP antibodies. The results showed that a high percentage of clonal populations were adipogenic (82%), osteogenic (64%) and neurogenic (79%) potential positive (Fig. 3). Of 20 clones analyzed, 17 clone-derived showed multilineage potential, as shown by their differentiation along several mesodermal and neural lineages.

pATSCs exhibit mesodermal lineage differentiation

pATSCs did not spontaneously differentiate during in vitro culture expansion. The differentiation potential of rhesus pATSCs appears very similar to human pATSCs (see Table 2) (Kang et al., 2003). Using lineage-specific differentiation culture media, expanded pATSCs were capable of generating adipocytes as indicated by the accumulation of neutral lipid vacuoles (Fig. 1E). Osteogenic lineage capacity was detected by an increase in calcium deposition, as identified by Alzarin Red S (Fig. 1F). Chondrogenic induction of pATSCs, under the micromass conditions, resulted in cell condensation after induction and was followed by spheroid or nodule formation by 3-4 weeks. Nodules at this time point stained positively using Safranin O staining solution. pATSCs chondrogenesis was absolutely dependent on high cell density and induction conditions (Fig. 1G). Bone nodule formation was dependent on the presence of TGFβ1 and could not be induced in monolayer cultures. To analyse clonally derived populations of pATSCs, we performed low density cell culture in 10-cm dishes (50-100 cells). More than 95% of the CFU derived from single cell differentiated to mesodermal lineages (adipogenic, osteogenic and chondrogenic) after 20 days in lineage specific induction

Table 2. Comparison of the in vitro differentiation capabilities of the pATSC and pBMSC cell lines

Cell type	pATSC	pBMSC
Adipocyte	+++	+++
Chondrocyte	+	–
Osteoblast	++	+++
Neuronal cell	++	+

Cells were cultured in inducive media as described in Materials and Methods. The ability to differentiate to the indicated cell types was scored as: –, no differentiation observed; +, number of cells differentiating was estimated to be less than 10 %; ++, number of cells differentiating was estimated to be between 10 and 20%; +++, more than 20% of cells were estimated to be differentiating.

media. The pATSCs retained their multilineage potential for as long as 7 weeks of culture (data not shown). Cumulative population doublings were measured with respect to passage number in multiple animal samples. Our data were consistent with the observed lag time upon initial culture; pATSCs underwent an average of three population doublings before the first passage. An average of 1.5-2 population doublings was observed on subsequent passages, and a linear relationship between cumulative population doubling and passage number was observed (Fig. 1H). After their initial plating at 200-300 cells/cm^2, the pATSCs adherent cells reached confluence within 1-2 weeks. No detectable loss of self-renewal capacity could be observed through passage 13 (2-3 months in culture), which is markedly different from rhesus pBMSC cells (B.A.B., unpublished observations).

Induction of neural cell lineage protein expression in pATSCs

pATSCs and pBMSCs were induced towards the neurogenic lineage through neurosphere formation and final differentiation on PDL-laminin-coated substrate in NB media that was supplemented with B27, basic fibroblast growth factor (bFGF) and epidermal growth factor (EGF). Neural differentiation was analyzed through the detection of the expression of neuronal markers (MAP2ab, Neu N and NF160), in addition to GFAP as a marker of astrocytes. During neurogenic induction in NB media, both cell populations undergo a marked morphological change from elongated fibroblast morphology to compact, spheroid bodies, which expand to larger spheroid bodies as the total cell number expands (Fig. 2A,E). After detachment of the spheroid bodies from substrate, neural induction was performed neural induction for 4 days through suspension culture in Petri dishes and then the intact NS or dissociated NS were layered on the PDL-laminin-coated chamber slide and cultured for an additional 10 days. As soon as the cells were layered on laminin coated surface, the spheroid cell mass began to adhere and spread across the growth surface, forming long chains of cellular processes (Fig. 2B,C,F,G) and, finally, the cell processes began to exhibit secondary branching with multiple extensions (Fig. 2D,H).

To fully characterize the pATSC-derived neurospheres further, we performed both immunocytochemistry and western blot analysis for specific antigens indicative of neural cell lineages. The data from these analyses indicate that pATSC-derived neurospheres express high levels of nestin, MAP2ab,

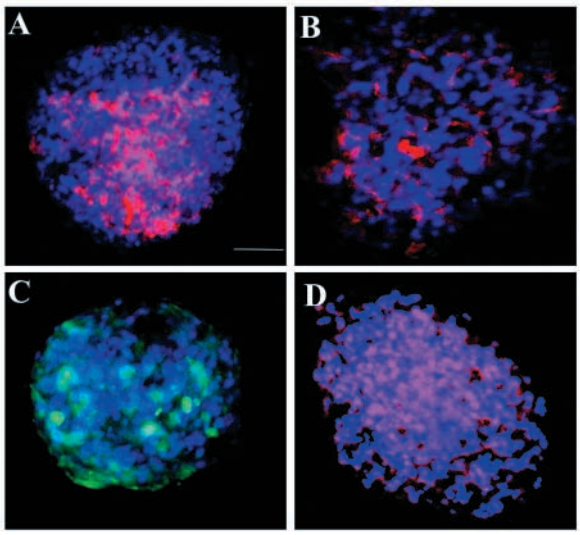

Fig. 4. Characterization of pATSCs-derived neurospheres pATSCs-NS. The pATSC-NS express nestin (A, red), and show strong expression of MAP2ab (B, red), GFAP (C, green) and CD133 (D, red). Blue color is DAPI staining. Bar, 60 μm (A-D).

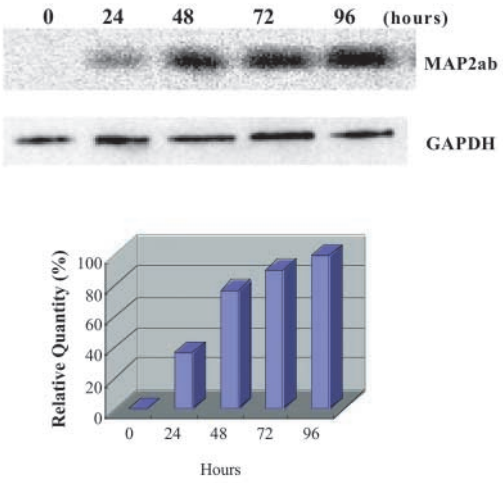

Fig. 5. Time course of MAP2ab expression of pATSC-NS. pATSC were detached from culture dish and cultured in suspension in NB medium supplemented with B27, bFGF, EGF. Each sample was isolated at a predetermined time period, and expression of MAP2ab was analyzed by western blot and quantitated. Maximum MAP2ab levels were detected at 4 days (96 hours), after which levels were downregulated. Control pATSCs do not express the MAP2ab protein.

GFAP and CD133 (Fig. 4A-D). We next assessed the levels and the pattern of induction of MAP2ab expression in pATSC-NS from 0 to 6 days of neurosphere formation. The results indicated that MAP2ab expression was significantly induced through the fourth day of NS formation and then decreased (Fig. 5). The decreased expression of MAP2ab protein may be derived from apoptosis or death of inner cells within the neurospheres. The pATSC-NS cells differentiated on the laminin-coated surfaces for 10 days. The increase in neural lineage related protein expression on neural induction was confirmed using RT-PCR analysis (Fig. 6), and double immunostaining for MAP2ab (Fig. 7A,E,F), Neu N (Fig. 7B,D), NF160 (Fig. 7A,B), astrocyte marker, GFAP (Fig. 7C), and nestin (Fig. 7G) as well as western blot analysis (Fig. 8A). We failed to detect the expression of MBP in any of these assays, suggesting that pATSCs did not differentiate into oligodendrocytes in vitro. Control populations of undifferentiated pATSCs did not express detectable levels of the assessed neuronal, oligodendrocyte or astrocyte protein markers, confirming the specificity of our neural differentiation methods and immunocytochemical staining protocol. However, RT-PCR analysis confirmed the expression of nestin in undifferentiated pATSCs. The expression of markers characteristic of more mature neuronal subtypes, choline acetyltransferase (ChAT) or GAD_{65}, was not observed in pATSCs by RT-PCR (Fig. 6).

For comparison of neural differentiation potential between pATSCs and pBMSCs, western blot analysis was performed using MAP2ab and nestin antibodies; real-time RT-PCR was carried out with a MAP2ab-specific primer and probe set. We detected very low levels of nestin protein expression in NS derived from pBMSCs, however, in pATSC-derived NS it was highly expressed (Fig. 8A). Quantitative RT-PCR analysis indicated that MAP2ab expression level in the NS differentiated from pATSCs were twofold higher than those of pBMSC-NS (Fig. 8B). After neural induction and differentiation, analysis indicated that both nestin and MAP2ab

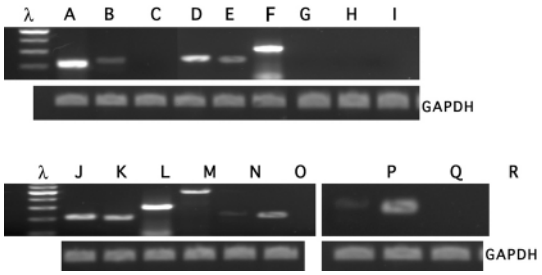

Fig. 6. RT-PCR analysis of stem cell and neural lineage marker expression in control pATSCs and differentiated pATSCs. Total cellular RNA (1 μg) was analyzed using the primers against several neural markers. The PCR product was separated on 1.5% agarose gel and visualized by ethidium bromide staining. Upper panel: undifferentiated pATSCs. λ, molecular marker; Lane A, Oct-4; Lane B, telomerase; Lane C, Hes1; Lane D, β-actin; Lane E, nestin; Lane F, BDNF; Lane G, MAP2ab; Lane H, GAD_{65}; Lane I, GFAP. Lower panel: Neuronal-lineage differentiated pATSCs. Lane J, Oct-4; Lane K, nestin; Lane L, BDNF; Lane M, MAP2ab; Lane N, GAD_{65}; Lane O, GFAP; Lane P, Trk A; Lane Q, Trk B; Lane R, P75.

were expressed at higher levels at both the RNA and protein levels in differentiated pATSCs than those in differentiated pBMSCs (Fig. 8).

Phenotypic analysis of pATSCs and pATSC-derived neurospheres

To explore the phenotypic characteristics of the isolated pATSCs, and pATSC-NS, we performed flow cytometry using primary antibodies against surface epitopes. The flow results indicated that undifferentiated pATSCs were negative for the hematopoietic markers CD3, CD4, CD8, CD34 or CD45. They do express the cell-surface epitopes CD13, CD90, CD59 and HLA-1, and very low levels of CD11b. Comparison of the flow

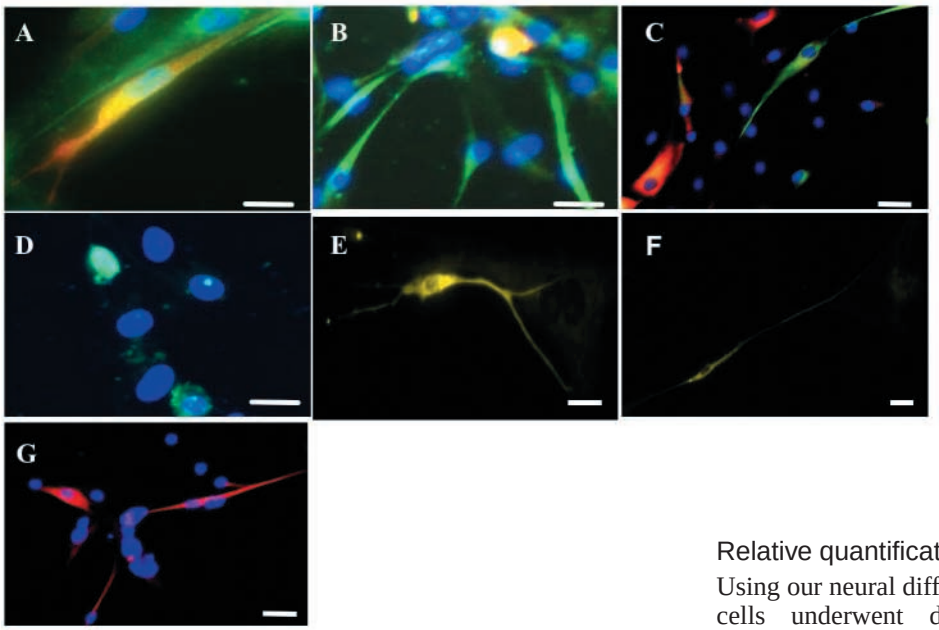

Fig. 7. Immunocytochemistry of pATSCs after neurosphere differentiation and culture on PDL-Laminin. Intense MAP2ab (A, red; E and F, yellow) and NF160 (A, green; B, green; C, green) expression and strong nuclear staining for Neu N (B, red; D, green) in pATSCs following neurosphere differentiation. High levels of GFAP (C, red), which is absent in undifferentiated pATSCs, were induced in after neurosphere differentiation. Prominent nestin (G, red) expression in cells derived from pATSC-derived neurospheres. Blue color is DAPI staining. Bars (A-G), 150 μm.

cytometric results for the undifferentiated rhesus pATSCs and pATSC-NS indicates that the expression of two CD marker antigens differ; CD90 (Thy-1) and CD164 (Sialomucin). Specifically, pATSC-derived neurospheres expressed high levels of CD90 and CD164, which were induced during neurosphere formation (Table 3).

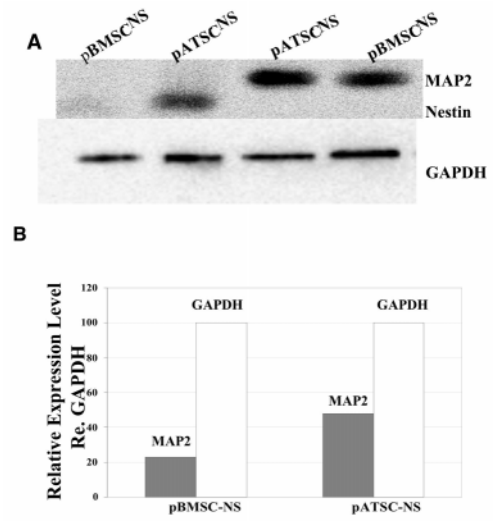

Fig. 8. Comparison of nestin and MAP-2 expression between neural differentiated pATSCs and pBMSCs. (A) Western blot analysis of whole cell lysate of fully differentiated pATSC and pBMSC-derived neurosphere (NS) maintained under neurobasal medium supplemented with B27, bFGF and EGF. Thirty micrograms of protein extract from each cell culture were separated on a 12% acrylamide gel and transferred to polyvinyldiethylfluoride (PVDF) membrane. The blots were probed with antibodies to nestin and MAP2ab followed by HRP-conjugated secondary antibody and developed using enhanced chemiluminescence. (B) Summary of the expression of the MAP2ab mRNA following NS differentiation, as quantified by real-time RT-PCR. The gene expression levels were normalized with respect to endogenous GAPDH.

Relative quantification of neural differentiated cells

Using our neural differentiation protocol, a variable number of cells underwent differentiation, although the response exceeded 70% of the starting population. In an attempt to optimize differentiation, we modified the neural differentiation protocol. The addition of BDNF (10 ng/ml) to the NB (supplemented medium B27, bFGF and EGF) increased the proportion of cells displaying neuronal characteristics and the response was more consistent (data not shown). After the incorporation of BDNF to the neural differentiation medium, neurotrophic factor receptor Trk B was induced in pATSCs-NS and differentiated pATSCs as indicated by RT-PCR analysis (Fig. 6, lane Q). Flow cytometric analysis of cells differentiated in the presence of BDNF showed that this cell population stained positive for the neuronal marker MAP2ab (53% positive cells), nestin (49%) and the astrocytic marker GFAP (55%) (Fig. 9).

Table 3. Phenotypic characterization of the adipose stromal cell from primate and drived neurosphere

		Expression level	
Name	Marker alternative name	pATSC	pATSC-NS
CD11b	Mac-1	+/–	+
CD3	T3	–	–
CD4	T4,L3T4	–	–
CD13	aminopeptidase N	+	+
CD8	T8,Lyt2,3	–/+	–
CD34	L-selectin	–	–
CD90	Thy-1	++	++++
CD164	MGC-24	–	+
CD133	AC133	–	–
CD59	protectin/MAC inhibition	++++	++++
HLA-1		++++	++++

Cells were harvested by trypsinization of the cell lines. The resulting single cell suspensions were labeled with flourescently labeled antibodies against the indicated surface markers and analyzed using flow cytometry. All cells analyzed behaved as a single population, i.e. the whole populations was positive or negative, only the expression levels of the markers varied. The expression level of the markers was scored as: –, no expression detected; –/+, only a small peak shift observed when compared to the control; +, expression was in the first decade of control; ++, expression was between one and two decades higher than control; +++, expression two to three decades higher than control; ++++, expression more than three decades higher than control.

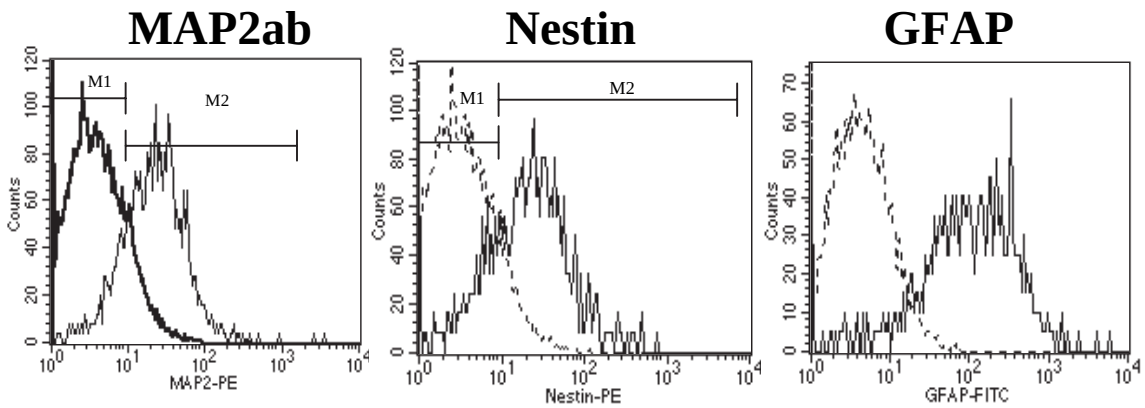

Fig. 9. Flow cytometry histograms of neural markers in neurospheres differentiated from pATSCs. Neurospheres were differentiated under supplemented NB medium for 10 days. The adherent cells were harvested and stained with monoclonal antibodies against GFAP coupled to fluorescein isothiocyanate (FITC) and nestin or MAP2ab coupled to phycoerythrin (PE). The distribution of pATSC-NS differentiated cells stained for those antibodies are shown. The geometric mean and median values for nestin, MAP2ab and GFAP are also shown.

Comparison of neural differentiation efficiency of the pATSCs and pBMSCs

We compared the in vitro neurogenic differentiation ability of pATSCs and pBMSCs. Neural lineage differentiation required that pATSCs and pBMSCs were cultured 1-2×10^4 cell/cm^2 in NB medium supplemented with B27. We also compared mesodermal lineage differentiation capability using lineage specific induction medium. The differentiation efficiency of these two cell types was more or less similar when induced along adipogenic and osteogenic lineages. However, pBMSCs did not undergo efficient chondrogenic differentiation under the conditions used in this study, suggesting distinctions in the differentiation capacities between pATSCs and pBMSCs (Table 1). Neuroprogenitors (Neurospheres) can be expanded with bFGF, EGF and BDNF, and more extensive differentiation induced by removal of cytokines and growth on PDL-laminin-coated surfaces. Populations of differentiated pATSCs and pBMSCs have morphological and phenotypical characteristics of astrocytes (GFAP), neurons (MAP2ab and NF60) and neuronal precursor cell marker (nestin). Cells positive for MBP (oligodendrocytic) were not generated in stem cells isolated from either adipose tissue or bone marrow. Quantitative RT-PCR analysis confirmed increased expression of BDNF in undifferentiated pATSCs compared with that in undifferentiated pBMSCs (data not shown).

Expressed gene profile of pATSC and pATSC-NS

In order to analyze the gene expression pattern, we performed oligonucleotide microarray analysis. The gene expression profile in pATSC control cells was compared with pATSC-NS. Total RNA was harvested from both cultures and gene expression profiles were compared using Affymetrix HG-U95a microarray (22,000 genes and ESTs). Affymetrix Microarray Suite 4.1 was used to scan and analyze the relative abundance of each gene. The signal output from each gene from the pATSC control profile was plotted against the pATSC-NS profile (Fig. 10), and the correlation coefficient (*r*) was calculated for each comparison. The analysis of the gene expression levels showed that less than 1% of the total genes were expressed at greater than 2.2-fold different levels in pATSC and pATSC-NS, as indicated by the *r* value (=0.8). In the online supplemental data, Table 4 shows a partial list of genes that are highly relevant for neural lineage development that were either induced (total number of genes=25) or inhibited (total number of genes=12) in differentiated pATSC-NS when compared with undifferentiated pATSC control cells. Table S1 (http://jcs.biologists.org/supplemental/) gives a partial list assembled into gene function of non-neuronal genes that are either upregulated (total number of genes=260) or downregulated (total number of genes=569) expressed in pATSC-NS compared with naïve pATSC.

Discussion

The data from this study show that cells with multipotent adult progenitor characteristics can be isolated from different organs

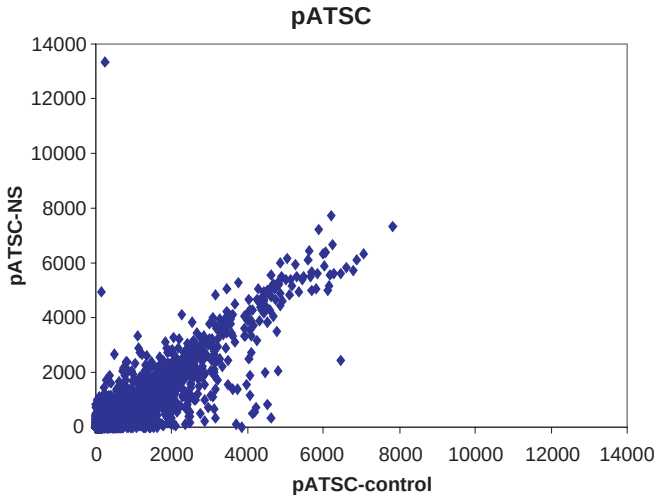

Fig. 10. Expressed gene profile in pATSC and pATSC-NS are similar. Scatter plot shows gene expression in pATSC and pATSC-NS. Template RNA was extracted from 3×10^6 cells derived from neurospheres. cDNA was prepared, labeled and hybridized to the Affymetrix HGU 95A2 array containing ~22,000 human genes. Data analysis was done using Genechip software.

Table 4. Important genes for neural lineage differently expressed in pATSC-NS

Genes	Accession no.	Locus link	Fold change
Midkine (neurite growth-promoting factor 2)	M69148.1	4192	7.92
Vascular endothelial growth factor	AF091352.1	7422	6.82
ret finger protein	AF230394.1	5987	3.27
HIF-1 responsive RTP801	NM-019058.1	54541	3.41
Cyclin T2	AV681875	905	4.53
Oncostatin M receptor	NM_003999	9180	4.27
Lectin, mannose-binding, 1	NM_005570.2	3998	2.69
Bone morphogenetic protein 1	NM_001199.1	649	3.21
Platelet derived growth factor C	NM_016205.1	56034	4.69
DEAD/H (Asp-Glu-Ala-Asp/His) box polypeptide 9 (RNA helicase A)	BE910323	1660	3.11
Pleckstrin homology-like domain, family A, member 1	AA576961	22822	3.1
Diazepam binding inhibitor (GABA receptor modulator, acyl-Coenzyme A binding protein)	M15887.1	1622	2.56
Cellular retinoic acid binding protein 2	NM_001878	1382	5.79
Transcription factor 12	AL_559478	6938	2.24
Survival of motor neuron protein interacting protein 1	NM_003616.1	8487	4.66
v-fos FBJ murine osteosarcoma viral oncogene homolog	BC004490.1	2353	5.16
v-maf musculoaponeurotic fibrosarcoma oncogene homolog B (avian)	NM_005461.1	9935	6.06
Zinc finger protein 133 (clone pHZ-13)	AL049646	7692	3.15
Uncharacterized hypothalamus protein HCDASE	NM_018479.1	55862	2.93
Adrenergic, α-2A-, receptor	AF284095.1	150	287.19
Transforming growth factor, β receptor I (activin A receptor type II-like kinase, 53 kDa)	NM_004612.1	7046	3.5
Thymosin, β, identified in neuroblastoma cells	BF_677486	11013	2.18
Transcription factor 8	U_19969.1	6935	4.05
Roundabout, axon guidance receptor, homolog 1 (*Drosophila*)	BF059159	6091	4.88
Syntaxin 1A (brain)	NM_004603.1	6804	6.48
Signal transducer and activator of transcription 1, 91 kDa	NM_007315.1	6772	–4.1
Latent transforming growth factor β binding protein 2	NM_000428.1	4053	–5.87
Cysteine-rich motor neuron 1	BG546884	51232	–12.43
Insulin-like growth factor binding protein 2, 36 kDa	NM_000597.1	3485	–38.95
Erythropoietin	AF053356	2056	–7.43
Nerve growth factor, β polypeptide	NM_002506.1	4803	–9.44
Dickkopf homolog 3 (*Xenopus laevis*)	NM_013253.1	27122	–4.46
Laminin, α4	NM_002290.2	3910	–4.51
Achaete-scute complex-like 1 (*Drosophila*)	BC001638.1	429	–15.64
Monoamine oxidase A	NM_000240.1	4128	–7.5
Gamma-aminobutyric acid (GABA) receptor, ρ1	NM_002042	2569	–14.64
5-Hydroxytryptamine (serotonin) receptor 2B	NM_000867.1	3357	–5.82

in non-human primates. The cells have similar morphology, phenotype and in vitro differentiation ability, and they have highly similar gene expression profiles (Wieczorek et al., 2003). Primary cultures of bone marrow and adipose tissue are a heterogeneous population containing small numbers of hematopoietic cells, pericytes, endothelial cells and smooth muscle cells (Zuk et al., 2001). However, Gronthos et al. reported that the frequency of these other cells appears to diminish quickly through serial passages in culture (Gronthos et al., 2001). Also, these cells have the ability to differentiate into multiple lineages, including osteogenic, adipogenic, chondrogenic and neural differentiation. We used pATSCs of 3-4 passages for the experiments and observed that more than 95% of cells expressed CD59 and HLA-1, but not CD34, CD3, CD4 or CD8. Also, the low levels of nestin and GFAP expression in undifferentiated ATSCs in the rhesus model are consistent with the previous reports in stromal cells of bone marrow origin (Deng et al., 2001; Kang et al., 2003) and suggest that ATSCs may retain a native potential for neural differentiation. pATSCs following the induction of neural differentiation revealed biologic and morphologic characteristics of neural lineages. The high percentage of cells undergoing neural differentiation in our study indicates that neural differentiation is occurring within a broad population of pluripotent cells. While immunocytochemical evidence from us and others (Zuk et al., 2001; Zuk et al., 2002) suggests that neurogenesis can occur in culture from rhesus adipose stromal cells, it remains to be investigated whether these neurons are electrically active and functional with all essential characteristics of mature CNS neurons (Song et al., 2002). In accordance with previous studies, stem and progenitor cells from adult adipose stromal tissue retain the capacity to differentiate toward mesenchymal and nonmesenchymal lineages, similar to bone marrow stromal cells (Sanchez-Ramos et al., 2000; Woodbury et al., 2000; Zuk et al., 2001; Erickson et al., 2002; Safford et al., 2002). Recent work on BMSCs undergoing early neurogenic differentiation has confirmed the expression of nestin, an intermediate filament protein thought to be expressed at high levels in neural stem cells (Sanchez-Ramos et al., 2000). Consistent with this, nestin expression was detected in noninduced pATSCs as well as in those induced under several neurogenic media conditions, suggesting the differentiation potential of pATSCs into a neural stem cell phenotype. Recently, nestin expression has also been observed in myogenic cells, endothelial cells and hepatic cells, indicating that it cannot be used as a marker for putative neurogenic differentiation of non-neural stem cells. After differentiation pATSCs showed a neuron-like morphology and the increased expression of three neuron specific proteins, NSE, MAP2ab and NF160 and mature astrocyte marker GFAP.

MAP2ab and Neu N expression is thought to coincide with terminal differentiation of pATSCs. Also, coexpression of Neu N, MAP2ab and early neural precursor marker nestin may indicate potential neurogenic capacity in pATSCs. Compared with pATSCs, neural-lineage-induced pBMSCs have lower levels of MAP2ab expression indicating that neural lineage potential of the pATSCs may be greater than that of pBMSCs.

Analysis of pATSCs and pBMSCs properties has identified many common biological characteristics between the two populations. Importantly, we have also observed several distinct properties in the two populations that suggest they are very similar but not identical (Table 1). Also, our cell culture experience with pATSCs indicates that screening lots of serum, a requirement for efficient pBMSC culture, is not necessary for efficient expansion and differentiation. Our data indicate that pBMSCs did not undergo chondrogenic differentiation under the conditions used in this study, suggesting distinct differentiation capacities between the two stem cell lineages. Immunocytochemical analysis also identified differences in the surface epitope profiles of pATSC and pBMSC populations, and our data and others indicate that these distinctions between ATSC and BMSC populations may also extend down to the gene level (Zuk et al., 2002). BDNF and MAP2ab real-time RT-PCR data showed that the neural differentiation capabilities of pATSCs may be significantly higher than those of pBMSCs.

The differentiation potential of pATSCs may result from the commitment of lineage-specific precursors rather than the presence of a multipotent stem cell population. To verify proliferation and differentiation potential of pATSCs, we isolated clones derived from single pATSCs cells in 96-well plates. After 14 days culture, the plates were stained with 0.5% crystal violet in methanol for 5 minutes and we counted the number of colonies that were more than 2 mm in diameter. Around 80-90% of single clone cultures generated crystal violet-positive CFU clones after high potency of self renewal. For evaluation of multipotency of pATSCs-derived single cell clones, we passaged cloned population to population doubling (PD) 100 to PD 150. Single clone-derived ATSCs were plated at 50 cell/cm^2 and cultured and induced to adipogenic, osteogenic and neurogenic lineage differentiation. A high percentage of clonal populations were demonstrated to retain adipogenic (82%), osteogenic (64%) and neurogenic (79%) differentation potential (Fig. 3). Of 20 clones analyzed, 17 clones showed pluripotential potency along several mesodermal and neural lineages. This result indicates that a high ratio of subpopulation of pATSCs have the characteristics of multipotential and pluripotential in vitro, because individual progenitor cells are capable of self-renewal and can generate daughter cells capable of differentiating into the major mesodermal and ectodermal lineage. It also showed that more than 75% of subpopulation of pATSCs had neurogenic potential.

To investigate patterns of gene expression during the process of neurosphere formation and culture, cDNA microarray analysis was performed. Labeled cDNA targets were hybridized with the microarray, and 829 clones (downregulated gene in pATSC-NS=569, unregulated gene in pATSC-NS=260) that differed by more than twofold intensity in at least one pairwise comparison were selected. That 22,000-gene microarray is representative of all the unique human gene sequences that were available at the time the array was produced. Many of the genes with the highest intensity values (Z score >8) in pATSC control and pATSC-NS were ESTs or unnamed genes. A discussion of all the named genes that were increased or decreased in the pATSC-NS related to pATSC control is impractical within the context of this paper. These include *oncostatin M receptor*, *HIF-1 responsive RTP801*, *PDGF C*, *cellular retinoic acid binding protein 2*, *TGF β receptor 1*, *and syntaxin 1A*. Furthermore, several genes including *insulin-like growth factor beta polypeptide*, *dickkopf homolog3*, *achaete-scute complex like 1*, *and erythropoietin* that are expressed in neural stem cells were highly downregulated in pATSC-NS compare with pATSC control. Table S1 (http://jcs.biologists.org/supplemental/) provides categories of genes that showed differences in expression levels (increased or decreased in pATSC-NS compared with pATSC) between two samples. Several genes that have been reported to be important for neural lineage were highly expressed in pATSC-NS (Table 3) (Wright et al., 2003). A broad variety of cellular functions are represented, including signaling, structural elements, cell cycle control and apoptosis, DNA function, transcription and translation, transport activity, cell adhesion, growth and trophic factors, general metabolic proteins and enzymes, as well as catalytic activity related genes. Because entire genome sequences or even large clustered EST sequences from many of the non-human primates used as experimental models in biomedical research are not currently available, interspecies microarray hybridization studies represent one possible way to identify genes within a transcriptome and profile the expression levels. The microarray technology platform used here in uniform and data can be normalized from different experiments (real-time RT-PCR, immunocytochemistry). Furthermore, in previous studies (Marketa et al., 2003), the proportion of common genes shared between humans and macaque species might be higher than between two different monkey species.

Adipose stromal cells are easily obtained from patients and are, therefore, one of the most clinically practical sources of stem cells in adults. Moreover, these cells have few practical, ethical or immunological barriers to their clinical application and are promising materials for future cell and gene therapies. Devine et al. (Devine et al., 2001) reported that the intravenous injection of mesenchymal stem cells into baboons (*papio anubis*) was not associated with significant toxicity and the cells were capable of homing to and establishing residence in the bone marrow for an extended period of time. Recently, transplantation of human ATSCs improved functional deficits in ischemic brain injury induced by MCAo (Kang et al., 2003). Intracerebral grafting of BDNF-transduced hATSCs significantly improved motor recovery of functional deficits in MCAo rats. The data from this study indicate that transplanted hATSCs survive, migrate and improve functional recovery after recovery of stroke, and that genetically engineered hATSCs can express biologically active gene products and, therefore, can function as effective vehicles for therapeutic gene transfer to the damaged brain.

In summary, we have identified and characterized non-human primate adipose tissue stromal cells that contain progenitor cells that have a potential for in vitro expansion and neural differentiation.

We are extremely grateful to Xavier Alvarez for his help with the confocal microscopy, and Louis Martin and the staff of the flow cytometry core laboratory for their help with flow cytometric analyses. We would also like to thank James Munoz for helpful discussions.

The work was supported by grant number RR00164 from the National Center for Research Resources, National Institutes of Health, a grant from the State of Louisiana Millennium Health Excellence Fund and the Louisiana Gene Therapy Research Consortium.

References

Azizi, S. A., Stokes, D., Augelli, B. J., DiGirolamo, C. and Prockop, D. J. (1998). Engraftment and migration of human bone marrow stromal cells implanted in the brains of albino rats: similarities to astrocyte grafts. *Proc. Natl. Acad. Sci. USA* **95**, 3908-3913.

Barami, K., Hao, H. N., Lotoczky, G. A., Diaz, F. G. and Lyman, W. D. (2001). Transplantation of human fetal brain cells into ischemic lesions of adult gerbil hippocampus. *J. Neurosurg.* **95**, 308-315.

Black, I. and Woodbury, D. (2001). Adult rat and human bone marrow stromal stem cells differentiate into neurons. *Blood Cells Mol. Dis.* **27**, 632-636.

Borlongan, C. V., Koutouzis, T. K., Jorden, J. R., Martinez, R., Rodriguez, A. I., Poulos, S. G., Freeman, T. B., McKeown, P., Cahill, D. W., Nishino, H. et al. (1997). Neural transplantation as an experimental treatment modality for cerebral ischemia. *Neurosci. Biobehav. Rev.* **21**, 79-90.

Brazelton, T. R., Rossi, F. M. V., Keshet, G. I. and Blau, H. M. (2000). From marrow to brain: expression of neuronal phenotypes in adult mice. *Science* **290**, 1775-1779.

Colter, D. C., Class, R., DiGirolamo, C. M. and Prockop, D. J. (2000). Rapid expansion of recycling stem cells in cultures of plastic-adherent cells from human bone marrow. *Proc. Natl. Acad. Sci. USA* **97**, 3213-3218.

Colter, D. C., Sekiya, I. and Prockop, D. J. (2001). Identification of a subpopulation of rapidly self-renewing and multipotential adult stem cells in colonies in human marrow stromal cells. *Proc. Natl. Acad. Sci. USA* **98**, 7841-7845.

Deng, W., Obrocka, M., Fischer, I. and Prockop, D. J. (2001). In vitro differentiation of human marrow stromal cells into early progenitors of neural cells by conditions that increase intracellular cyclic AMP. *Biochem. Biophys. Res. Commun.* **282**, 148-152.

Devine, S. M., Bartholomew, A. M., Mahmud, N., Nelson, M., Patil, S., Hardy, W., Sturgeon, C., Hewett, T., Chung, T., Stock, W. et al. (2001). Mesenchymal stem cells are capable of homing to the bone marrow of non-human primates following systemic infusion. *Exp. Hematol.* **29**, 244-255.

Ding, L., Lu, S., Batchu, R. B., Saylors, R. L. and Munshi, N. C. (1999). Bone marrow stromal cells as a vehicle for gene transfer. *Gene Ther.* **6**, 1611-1616.

Erickson, G. R., Gimble, J. M., Franklin, D. M., Rice, H. E., Awad, H. and Guilak, F. (2002). Chondrogenic potential of adipose tissue-derived stromal cells in vitro and in vivo. *Biochem. Biophys. Res. Commun.* **290**, 763-769.

Gronthos, S., Franklin, D. M., Leddy, H. A., Robey, P. G., Storms, R. W. and Gimble, J. M. (2001). Surface protein characterization of human adipose tissue-derived stromal cells. *J. Cell. Physiol.* **189**, 54-63.

Gussoni, E., Soneoka, Y., Strickland, C. D., Buzney, E. A., Khan, M. K., Flint, A. F., Kunkel, L. M. and Mulligan, R. C. (1999). Dystrophin expression in the *mdx* mouse restored by stem cell transplantation. *Nature* **401**, 390-394.

Halvorsen, Y. D., Bond, A., Sen, A., Franklin, D. M., Lea-Currie, Y. R., Sujkowski, D., Ellis, P. N., Wilkison, W. O. and Gimble, J. M. (2001). Thiazolidinediones and glucocorticoids synergistically induce differentiation of human adipose tissue stromal cells: biochemical, cellular, and molecular analysis. *Metabolism* **50**, 407-413.

Jin, H. K., Carter, J. E., Huntley, G. W. and Schuchman, E. H. (2002). Intracerebral transplantation of mesenchymal stem cells into acid sphingomyelinase-deficient mice delays the onset of neurological abnormalities and extends their life span. *J. Clin. Invest.* **109**, 1183-1191.

Kang, S. K., Lee, D. H., Bae, Y. C., Kim, H. K., Baik, S. Y. and Jung, J. S. (2003). Improvement of neurological deficits by intracerebral transplantation of human adipose tissue-derived stromal cells after cerebral ischemia in rats. *Exp. Neurol.* **183**, 355-366.

Kohyama, J., Abe, H., Shimazaki, T., Koizumi, A., Nakashima, K., Gojo, S., Taga, T., Okano, H., Hata, J. and Umezawa, A. (2001). Brain from bone: efficient "meta-differentiation" of marrow stroma-derived mature osteoblasts to neuron with Noggin or a demethylating agent. *Differentiation* **68**, 235-244.

Kopen, G. C., Prockop, D. J. and Phinney, D. G. (1999). Marrow stromal cells migrate throughout forebrain and cerebellum, and they differentiate into astrocytes after injection into neonatal mouse brains. *Proc. Natl. Acad. Sci. USA* **96**, 10711-10716.

Marketa, M., Jean, M., Edwan, B., Ronald, E. B., Laurent, P. and Garry, W. (2003). Microarray analysis of nonhuman primates: validation of experimental models in neurological disorders. *FASEB J.* **17**, 929-931.

Masada, T., Itano, T., Fujisawa, M., Miyamoto, O., Tokuda, M., Matsui, H., Nagao, S. and Hatase, O. (1997). Embryonic transplantation and ischemic memory deficit. *Neurosci. Res.* **27**, 249-255.

Mezey, E., Chandross, K. J., Harta, G., Maki, R. A. and McKercher, S. R. (2000). Turning blood into brain: cells bearing neuronal antigens generated in vivo from bone marrow. *Science* **290**, 1779-1782.

Park, K. W., Eglitis, M. A. and Mouradian, M. M. (2001). Protection of nigral neurons by GDNF-engineered marrow cell transplantation. *Neurosci. Res.* **40**, 315-323.

Patrick, C. W. (2000). Adipose tissue engineering: the future of breast and soft tissue reconstruction following tumor resection. *Semin. Surg. Oncol.* **19**, 302-311.

Petersen, B. E., Bowen, W. C., Patrene, K. D., Mars, W. M., Sullivan, A. K., Murase, N., Boggs, S. S., Greenberger, J. S. and Goff, J. P. (1999). Bone marrow as a potential source of hepatic oval cells. *Science* **284**, 1168-1170.

Reyes, M. and Verfaillie, C. M. (2001). Characterization of multipotent adult progenitor cells, a subpopulation of mesenchymal stem cells. *Ann. New York Acad. Sci.* **938**, 231-235.

Safford, K. M., Hicok, K. C., Safford, S. D., Halvorsen, Y. D., Wilkison, W. O., Gimble, J. M. and Rice, H. E. (2002). Neurogenic differentiation of murine and human adipose-derived stromal cells. *Biochem. Biophys. Res. Commun.* **294**, 371-379.

Sanchez-Ramos, J., Song, S., Cardozo-Pelaez, F., Hazzi, C., Stedeford, T., Willing, A., Freeman, T. B., Saporta, S., Janssen, W., Patel, N. et al. (2000). Adult bone marrow stromal cells differentiate into neural cells in vitro. *Exp. Neurol.* **164**, 247-256.

Sanchez-Ramos, J., Song, S., Kamath, S. G., Zigova, T., Willing, A., Cardozo-Pelaez, F., Stedeford, T., Chopp, M. and Sanberg, P. R. (2001). Expression of neural markers in human umbilical cord blood. *Exp. Neurol.* **171**, 109-115.

Shetty, A. K. and Turner, D. A. (1996). Development of fetal hippocampal grafts in intact and lesioned hippocampus. *Prog. Neurobiol.* **50**, 597-653.

Song, H. J., Stevens, C. F. and Gage, F. H. (2002). Neural stem cells from adult hippocampus develop essential properties of functional CNS neurons. *Nat. Neurosci.* **5**, 438-445.

Suzuki, K., Oyama, M., Faulcon, L., Robbins, P. D. and Niyibizi, C. (2000). In vivo expression of human growth hormone by genetically modified murine bone marrow stromal cells and its effect on the cells in vitro. *Cell Transplant.* **9**, 319-327.

Terskikh, A. V., Easterday, M. C., Li, L., Hood, L., Kornblum, M. K., Geschwind, D. H. and Weissman, I. L. (2001). From hematopoiesis to neuropoiesis: evidence of overlapping genetic programs. *Proc. Natl. Acad. Sci. USA* **98**, 7934-7939.

Wie, G., Schubiger, G., Harder, F. and Muller, A. M. (2000). Stem cell plasticity in mammals and transdetermination in *Drosophila*: common themes? *Stem Cells* **18**, 409-414.

Weissman, I. L. (2000). Translating stem and progenitor cell biology to the clinic: barriers and opportunities. *Science* **287**, 1442-1446.

Wieczorek, G., Steinhoff, C., Schulz, R., Scheller, M., Vingron, M., Ropers, H. H. and Nuber, U. A. (2003). Gene expression profile of mouse bone marrow stromal cells determined by cDNA microarray analysis. *Cell Tissue Res.* **311**, 227-237.

Woodbury, D., Schwarz, E. J., Prockop, D. J. and Black, I. B. (2000). Adult rat and human bone marrow stromal cells differentiate into neurons. *J. Neurosci. Res.* **61**, 364-370.

Woodbury, D., Reynolds, K. and Black, I. B. (2002). Adult bone marrow stromal stem cells express germline, ectodermal, endodermal, and mesodermal genes prior to neurogenesis. *J. Neurosci. Res.* **96**, 908-917.

Wright, L. S., Li, J., Caldwell, M. A., Wallace, K., Johnson, J. A. and Svendsen, C. N. (2003). Gene expression in human neural stem cells; effects of leukemia inhibitory factor. *J. Neurochem.* **86**, 179-195.

Zuk, P. A., Zuh, M., Mizuno, H., Huang, J., Futrell, J. W., Katz, A. J., Benhaim, P., Lorenz, H. P. and Hedrick, M. H. (2001). Multilineage cells from human adipose tissue: implications for cell-based therapies. *Tissue Eng.* **7**, 211-228.

Zuk, P. A., Zhu, M., Ashjian, P., de Ugarte, D. A., Huang, J. I., Mizuno, H., Alfonso, Z. C., Fraser, J. K., Benhaim, P. and Medrick, M. H. (2002). Human adipose tissue is a source of multipotent stem cells. *Mol. Biol. Cell* **13**, 4279-4295.

Table S1(A). Genes showed increase in pATSC-derived NS

Genes	Accession no.	Locus link	Fold change
"Regulations of cell cycle and fate" genes			
BUB3 budding uninhibited by benzimidazoles 3 homolog (yeast)	AU160695	9184	2.88
Adenovirus 5 E1A binding protein	NM_006624.1	10771	3.38
Retinoblastoma binding protein 8	NM_002894.1	5932	3.48
Topoisomerase (DNA) II alpha 170kDa	NM_001067.1	7153	7.39
Oxysterol binding protein-like 3	AI202969	26031	7.6
Replication factor C (activator 1) 3, 38kDa	BC000149.2	5983	2.87
Nijmegen breakage syndrome 1 (nibrin)	AK001017.1	4683	9.1
Osteoblast specific factor 2 (fasciclin I-like)	D13665.1	10631	3.15
Likely ortholog of mouse hepatoma-derived growth factor, related protein 3	AB029156.1	50810	3.22
T-box 3 (ulnar mammary syndrome)	NM_016569.1	6926	3.48
Hsp90-associating relative of Cdc37	NM_017913.1	55664	7.25
Adipose differentiation-related protein	BC005127.1	123	9.63
Interferon regulatory factor 2	NM_002199.2	3660	2.52
GM2 ganglioside activator protein	X61094.1	2760	4.19
Programmed cell death 4 (neoplastic transformation inhibitor)	NM_014456.1	27250	3.58
Protein phosphatase 1, regulatory (inhibitor) subunit 2	NM_006241.1	5504	2.87
IQ motif containing GTPase activating protein 1	AI679073	8826	2.86
Sparc/osteonectin, cwcv and kazal-like domains proteoglycan (testican)	AF231124.1	6695	25.83
Enolase 1, (alpha)	U88968.1	2023	3.25
"Nucleotide binding and general binding" genes			
Signal recognition particle receptor ('docking protein')	BG474541	6734	5.63
ATP-binding cassette, sub-family B (MDR/TAP), member 1	AF016535.1	5243	3.05
SWI/SNF related, matrix associated, actin dependent regulator of chromatin	AW131754	6595	3.73
RNA helicase-related protein	BF246115	11325	3.68
Chromobox homolog 3 (HP1 gamma homolog, Drosophila)	BE748755	11335	3.33
Nuclear receptor subfamily 4, group A, member 2	NM_006186.1	4929	4.17
Homeo box B7	NM_004502.1	3217	3.1
Histone 1, H4c	NM_003542.2	8364	4.23
Paired mesoderm homeo box 1	NM_006902.2	5396	6.66
High mobility group AT-hook 1	NM_002131.1	3159	2.84
ets variant gene 1	NM_004956.1	2115	3.8
Transcriptional co-activator with PDZ-binding motif (TAZ)	AA081084	25937	4.55
Dermatopontin	NM_001937.2	1805	22.71
Calcium binding protein P22	NM_007236.1	11261	3.79
Paxillin	D86862.1	5829	2.93
Gelsolin (amyloidosis, Finnish type)	BE675337	2934	3.76
Sarcomeric muscle protein	NM_006063.1	10324	3.33
NS1-binding protein	AB020657.1	10625	5.88
Procollagen C-endopeptidase enhancer	NM_002593.2	5118	3.74
Immunoglobulin superfamily containing leucine-rich repeat	NM_005545.1	3671	4.56
T-LAK cell-originated protein kinase	NM_018492.1	55872	4.18
Hsp90-associating relative of Cdc37	NM_017913.1	55664	7.25
"Cell fraction" genes			
Progesterone receptor membrane component 1	AL547946	10857	3.1
Mitochondrial ribosomal protein L15	NM_014175.1	29088	2.72
Conserved gene amplified in osteosarcoma	AF022231.1	10106	2.72
Oxidised low density lipoprotein (lectin-like) receptor 1	AF035776.1	4973	3.08
Cytochrome P450, family 24, subfamily A, polypeptide 1	NM_000782.1	1591	3.99
Cytochrome P450 retinoid metabolizing protein	NM_019885.1	56603	3.01
Fatty-acid-Coenzyme A ligase, long-chain 4	NM_022977.1	2182	3.02
GM2 ganglioside activator protein	X61094.1	2760	4.19
Hippocalcin-like 1	NM_002149.1	3241	4.26
Coronin, actin binding protein, 2B	BF939649	10391	4.3
"Catalytic activity" genes			
Protein kinase C, nu	Z25429.1	23683	3.77
PTK9 protein tyrosine kinase 9	NM_002822.1	5756	2.91
Protein tyrosine phosphatase type IVA, member 1	BF576710	7803	3.62
Pyruvate dehydrogenase phosphatase	NM_018444.1	54704	5.9
Ubiquitin specific protease 1	AW499935	7398	2.86
Fatty-acid-Coenzyme A ligase, long-chain 4	NM_022977.1	2182	3.02
Crystallin, zeta (quinone reductase)	NM_001889.1	1429	2.87
Aldehyde dehydrogenase 1 family, member A3	NM_000693.1	220	3.87
Peptidylprolyl isomerase D (cyclophilin D)	AI014573	5481	2.7
Sialyltransferase	NM_006456.1	10610	2.96
RAB, member of RAS oncogene family-like 4	NM_006860.2	11020	2.89
Glutaminyl-peptide cyclotransferase (glutaminyl cyclase)	NM_012413.2	25797	3.03
Proprotein convertase subtilisin/kexin type 5	NM_006200.1	5125	3.36
Hyaluronan synthase 2	NM_005328.1	3037	7.74
ATP-binding cassette, sub-family B (MDR/TAP), member 4	NM_000443.2	5244	3.93
Prion protein interacting protein	BC001072.1	79033	3.04
Phospholipase A2, group IVA (cytosolic, calcium-dependent)	M68874.1	5321	7.73

Catalase	AY028632.1	847	3.26
Methylthioadenosine phosphorylase	AF216650.1	4507	4.01
RAB7, member RAS oncogene family-like 1	BG338251	8934	3.71
F-box only protein 5	NM_012177.1	26271	2.96
T-LAK cell-originated protein kinase	NM_018492.1	55872	4.18
Ectonucleotide pyrophosphatase/phosphodiesterase 1	NM_006208.1	5167	3.47
"Signal transducer activity" genes			
Regulator of G-protein signalling 14	AF037195	10636	2.71
Progesterone receptor membrane component 1	AL547946	10857	3.1
Lymphocyte-specific protein 1	NM_002339.1	4046	6.38
Nuclear receptor subfamily 4, group A, member 2	NM_006186.1	4929	4.17
Ras-GTPase activating protein SH3 domain-binding protein 2	NM_012297.1	9908	3.29
PTK9 protein tyrosine kinase 9	NM_002822.1	5756	2.91
Oxidised low density lipoprotein (lectin-like) receptor 1	AF035776.1	4973	3.08
Caspase recruitment domain family, member 10	AY028896.1	29775	3.22
MAD, mothers against decapentaplegic homolog 1 (Drosophila)	U54826.1	4086	2.81
Docking protein 1, 62kDa (downstream of tyrosine kinase 1)	AF180527.1	1796	2.7
Mouse Mammary Turmor Virus Receptor homolog 1	BF974389	23625	2.9
Coatomer protein complex, subunit alpha	AI621079	1314	3.52
Pre-B-cell colony-enhancing factor	NM_005746.1	10135	2.8
Lamin B receptor	NM_002296.1	3930	3.36
Signal recognition particle receptor ('docking protein')	BG474541	6734	5.63
Coxsackie virus and adenovirus receptor	NM_001338.1	1525	5.66
Nuclear receptor subfamily 3, group C, member 1 (glucocorticoid receptor)	X03348.1	2908	3.28
START domain containing 13	AA128023	90627	3.09
Pre-B-cell colony-enhancing factor	NM_005746.1	10135	2.8
"Cell adhesion molecule activity" genes			
Membrane metallo-endopeptidase (neutral endopeptidase, enkephalinase,	AI433463	4311	4.12
Matrix metalloproteinase 11 (stromelysin 3)	NM_005940.2	4320	13.85
Integrin, beta 2 (antigen CD18 (p95), lymphocyte function-associated antigen	NM_000211.1	3689	7.09
Integrin, alpha 2 (CD49B, alpha 2 subunit of VLA-2 receptor)	NM_002203.2	3673	3.15
Fibronectin 1	AJ276395.1	2335	5.97
CD99 antigen	U82164.1	4267	3.02
Laminin, beta 1	NM_002291.1	3912	2.92
Vascular cell adhesion molecule 1	NM_001078.1	7412	2.83
Sushi-repeat-containing protein, X chromosome	NM_006307.1	8406	3.91
KIT ligand	NM_000899.1	4254	6.1
Dermatopontin	NM_001937.2	1805	22.71
Gelsolin (amyloidosis, Finnish type)	BE675337	2934	3.76
"Transporter activity" genes			
Ferredoxin 1	NM_004109.2	2230	4.15
Coated vesicle membrane protein	NM_006815.1	10959	3.26
Ras-GTPase activating protein SH3 domain-binding protein 2	NM_012297.1	9908	3.29
ATP-binding cassette, sub-family B (MDR/TAP), member 4	NM_000443.2	5244	3.93
Solute carrier family 25 (carnitine/acylcarnitine translocase), member 20	BC001689.1	788	3.05
Phospholipid transfer protein	NM_006227.1	5360	2.85

Table S2(B). Genes showed decrease in pATSC-derived NS

Genes	Accession no.	Locus link	Fold change
"Regulation of cell cycle and cytokine" genes			
Interleukin 8	NM_000584.1	3576	–7.97
Cell division cycle 2-like 5 (cholinesterase-related cell division controller)	AJ297710.1	8621	–7.63
Candidate mediator of the p53-dependent G2 arrest	NM_019845.1	56475	–5.85
Growth arrest and DNA-damage-inducible, beta	NM_015675.1	4616	–6.95
WAP four-disulfide core domain 1	NM_021197.1	58189	–20.48
ATPase, H+ transporting, lysosomal 42kDa, V1 subunit C, isoform 1	NM_001695.1	528	–9.8
Somatostatin	NM_001048.1	6750	–72.02
Cardiotrophin-like cytokine	NM_013246.1	23529	–12
Connective tissue growth factor	M92934.1	1490	–4.43
Prostate differentiation factor	AF003934.1	9518	–38.03
Rac/Cdc42 guanine nucleotide exchange factor (GEF) 6	D25304.1	9459	–44.22
SH3-domain binding protein 4	AF015043.1	23677	–4.12
Basic transcription element binding protein 1	NM_001206.1	687	–4.26
Transducin-like enhancer of split 1 (E(sp1) homolog, Drosophila)	AI951720	7088	–6.43
Mediator of RNA polymerase II transcription, subunit 6 homolog (yeast)	AF074723.1	10001	–7.82
Heat shock 27kDa protein family, member 7 (cardiovascular)	NM_014424.1	27129	–4.62
Heat shock 70kDa protein 2	U56725.1	3306	–5
Hemochromatosis	BG402460	3077	–61.62
met proto-oncogene (hepatocyte growth factor receptor)	X54559.1	4233	–14.74
Chondroitin sulfate proteoglycan 4 (melanoma-associated)	BE857703	1464	–6.69
runt-related transcription factor 2	L40992.1	860	–6.91
"Intracellular" genes			
CD24 antigen (small cell lung carcinoma cluster 4 antigen)	L33930	934	–8.31
Apolipoprotein M	NM_019101.1	55937	–5.04
Lymphocyte antigen 6 complex, locus H	NM_002347.1	4062	–6.57
Oxysterol binding protein-like 1A	NM_018030.1	114876	–4.94
Antigen identified by monoclonal antibody MRC OX-2	H23979	4345	-17.84
Monocyte to macrophage differentiation-associated	NM_012329.1	23531	–5.13
CD151 antigen	NM_004357.1	977	–6.8
Fatty acid binding protein 3, muscle and heart	NM_004102.2	2170	–73.07
DnaJ (Hsp40) homolog, subfamily C, member 1	NM_022365.1	64215	–4.47
Serum deprivation response (phosphatidylserine binding protein)	NM_004657.1	8436	–10.95
"Extracelluar membrane protein and cellular morphogenesis" genes			
EGF-containing fibulin-like extracellular matrix protein 1	AI826799	2202	–9.61
Fibromodulin	NM_002023.2	2331	–12.24
Fibrinogen-like 2	NM_006682.1	10875	–5.46
Aggrecan 1 (chondroitin sulfate proteoglycan 1)	NM_001135.1	176	–38.48
Microfibril-associated glycoprotein-2	U37283.1	8076	–6.12
Secreted phosphoprotein 1 (osteopontin, bone sialoprotein I	M83248.1	6696	–11.57
A disintegrin-like and metalloprotease (reprolysin type)	AK023795.1	9510	–5.46
Cathepsin H	NM_004390.1	1512	–5.2
Dystrophin (muscular dystrophy, Duchenne and Becker types)	NM_004010.1	1756	–18.19
A disintegrin and metalloproteinase domain 19 (meltrin beta)	Y13786.2	8728	–4.21
Matrix metalloproteinase 1 (interstitial collagenase)	NM_002421.2	4312	–15.41
Proline arginine-rich end leucine-rich repeat protein	NM_002725.1	5549	–18.46
Collagen, type XI, alpha 1	NM_001854.1	1301	–19.23
Milk fat globule-EGF factor 8 protein	BC003610.1	4240	–5.79
Junctional adhesion molecule 2	NM_021219.1	58494	–12.68
Melanoma cell adhesion molecule	M28882.1	4162	–12.11
Keratin 18	NM_000224.1	3875	–17.17
Matrix Gla protein	NM_000900.1	4256	–6.02
Titin	NM_003319.1	7273	–3.94
Keratin 7	BC002700.1	3855	–37.14
Crystallin, alpha B	AF007162.1	1410	–280.07
Microfibril-associated glycoprotein-2	U37283.1	8076	–6.12
Arg/Abl-interacting protein ArgBP2	NM_021069.1	8470	–6.72
SWI/SNF related, matrix associated, actin dependent regulator of chromatin	AA593983	6599	–4.52
Inhibitor of DNA binding 4, dominant negative helix-loop-helix protein	NM_001546.1	3400	–13
Inhibitor of DNA binding 3, dominant negative helix-loop-helix protein	NM_002167.1	3399	–5.93
Heat shock 27kDa protein family, member 7 (cardiovascular)	NM_014424.1	27129	–4.62
"Motor activity and actin binding" genes			
Actin, alpha 2, smooth muscle, aorta	NM_001613.1	59	–8.4
Actin, gamma 2, smooth muscle, enteric	NM_001615.2	72	–9.78
Tropomyosin 1 (alpha)	Z24727.1	7168	–6.06
Calponin 1, basic, smooth muscle	NM_001299.1	1264	–15.55
Smoothelin	NM_006932.1	6525	–4.93
Myosin, heavy polypeptide 2, skeletal muscle, adult	NM_017534.1	4620	–39.58
Myosin, heavy polypeptide 11, smooth muscle	AI889739	4629	–39.78
Myosin, light polypeptide 9, regulatory	NM_006097.1	10398	–4.75
Myosin regulatory light chain interacting protein	NM_013262.2	29116	–9.88
Troponin C, slow	AF020769.1	7134	–17.54
Elastin (supravalvular aortic stenosis, Williams-Beuren syndrome)	AA479278	2006	–5.3
Dystrophin (muscular dystrophy, Duchenne and Becker types)	NM_004010.1	1756	–18.19
Caldesmon 1	AL577531	800	–4.48

Myosin, heavy polypeptide 1, skeletal muscle, adult	NM_005963.2	4619	–38.43
Myosin, heavy polypeptide 10, non-muscle	AI382123	4628	–55.87
Cardiac ankyrin repeat protein	NM_014391.1	27063	–110.38
Filamin C, gamma (actin binding protein 280)	NM_001458.1	2318	–3.92
Filamin B, beta (actin binding protein 278)	M62994.1	2317	–6.03
Dishevelled associated activator of morphogenesis 1	AK021890.1	23002	–6.36
"Catalytic activity" genes			
Creatine kinase, brain	NM_001823.1	1152	–6.59
Transglutaminase 2	AL031651	7052	–14.55
ATPase, Na+/K+ transporting, beta 1 polypeptide	NM_001677.1	481	–5.72
Serum/glucocorticoid regulated kinase	NM_005627.1	6446	–5.72
Peptidylprolyl isomerase F (cyclophilin F)	BC005020.1	10105	–7.37
Phosphoprotein regulated by mitogenic pathways	NM_025195.1	10221	–4.45
Dimethylarginine dimethylaminohydrolase 1	AL078459	23576	–5.84
Serine (or cysteine) proteinase inhibitor, clade E	NM_000602.1	5054	–5.26
Phosphoenolpyruvate carboxykinase 2 (mitochondrial)	NM_004563.1	5106	–4.2
ATPase, H+ transporting, lysosomal 42kDa, V1 subunit C, isoform 1	NM_001695.1	528	–9.8
Glutaminase	AF097493.1	2744	–5.82
Sulfotransferase family, cytosolic, 1A, phenol-preferring, member 1	NM_001055.1	6817	–4.08
Sulfotransferase family, cytosolic, 1A, phenol-preferring, member 2	NM_001054.1	6799	–4
Sulfotransferase family, cytosolic, 1A, phenol-preferring, member 3	U08032.1	6818	–4.16
Heme oxygenase (decycling) 1	NM_002133.1	3162	–5.92
Phosphoenolpyruvate carboxykinase 2 (mitochondrial)	NM_004563.1	5106	–4.2
Aldehyde dehydrogenase 3 family, memberA1	NM_000691.1	218	–63.06
Cell division cycle 2-like 5 (cholinesterase-related cell division controller)	AJ297710.1	8621	–7.63
Paired basic amino acid cleaving system 4	NM_002570.1	5046	–7.56
Ectonucleotide pyrophosphatase/phosphodiesterase 2 (autotaxin)	L35594.1	5168	–16.94
Monoglyceride lipase	BC006230.1	11343	–4.08
Sulfatase 1	AW043713	23213	–5.79
Protein phosphatase 2 (formerly 2A), regulatory subunit B (PR 52)	AA974416	5521	–17.35
Dual oxidase 1	AL137592.1	53905	–14.96
Tumor endothelial marker 6	NM_022748.1	64759	–4.21
ATP-binding cassette, sub-family A (ABC1), member 7	NM_019112.1	10347	–5.56
UDP glycosyltransferase 1 family, polypeptide A8	NM_019076.1	54576	–4.88
"Receptor activity" genes			
Dachshund homolog (Drosophila)	AW772082	1602	–82.27
Growth hormone receptor	NM_000163.1	2690	–4.67
G protein-coupled receptor, family C, group 5, member B	NM_016235.1	51704	–4.97
Cardiac ankyrin repeat protein	NM_014391.1	27063	–110.38
Diphtheria toxin receptor (heparin-binding epidermal growth factor)	NM_001945.1	1839	–4.32
Bone morphogenetic protein receptor, type II (serine/threonine kinase)	U20165.1	659	–4.19
G protein-coupled receptor 51	AF056085.1	9568	–5.54
Mediator of RNA polymerase II transcription, subunit 6 homolog (yeast)	AF074723.1	10001	–7.82
met proto-oncogene (hepatocyte growth factor receptor)	X54559.1	4233	–14.74
Toll-like receptor 4	NM_003266.1	7099	–4.37
"Transporter activity" genes			
Solute carrier family 24 (sodium/potassium/calcium exchanger), member 3	R62432	57419	–4.33
Aquaporin 1 (channel-forming integral protein, 28kDa)	NM_004102.2	2170	–73.07
lipocalin 2 (oncogene 24p3)	AL518391	358	–4.46
"Protein tyrosine kinase activity" genes			
Wingless-type MMTV integration site family, member 4	NM_005564.1	3934	–4.43
LIM protein (similar to rat protein kinase C-binding enigma)	NM_030761.1	54361	–24.04
Nephroblastoma overexpressed gene	BF671400	10611	–5.36
RAS protein activator like 2	BF440025	4856	–23.92
Tenascin C (hexabrachion)	D25304.1	9459	–44.22
Serum/glucocorticoid regulated kinase	NM_002160.1	3371	–4.83
Phosphoprotein regulated by mitogenic pathways	NM_005627.1	6446	–5.72
Fibromodulin	NM_025195.1	10221	–4.45
Pleiomorphic adenoma gene 1	NM_002023.2	2331	–12.24
Oxysterol binding protein-like 1A	NM_002655.1	5324	–6.7
Caldesmon 1	NM_018030.1	114876	–4.94